models for turbulent flows: LES

LES

(1) $$\mathbf{u}(\mathbf{x},t) = \mathbf{u}_F + \mathbf{u}_S$$

(2) $$\mathbf{u}_F(\mathbf{x},t) = \int G(\mathbf{r},\mathbf{x})\mathbf{u}(\mathbf{x}-\mathbf{r},t)\,\mathrm{d}^3\mathbf{r}$$

(3) $$\int G(\mathbf{r},\mathbf{x})\,\mathrm{d}^3\mathbf{r} = 1$$

Homogeneous filter: $G(\mathbf{r})$: filtering and differentiation commute.

Box filter

Deardorff (1970): $\Delta = (\Delta_1\ \Delta_2\ \Delta_3)^{1/3}$.

(4) $$\mathbf{u}_F(\mathbf{x},t) = \frac{1}{\Delta_1\Delta_2\Delta_3}\int_{x_1-\Delta_1/2}^{x_1+\Delta_1/2}\int_{x_2-\Delta_2/2}^{x_2+\Delta_2/2}\int_{x_3-\Delta_3/2}^{x_3+\Delta_3/2}\mathbf{u}(\mathbf{x}',t)\,\mathrm{d}x_1'\,\mathrm{d}x_2'\,\mathrm{d}x_3'$$

(5) $$G(\mathbf{r}) = \frac{1}{\Delta^3}\prod_{i=1}^{3}\mathrm{H}(\Delta_i/2-|r_i|)$$

Note that the average over the box

(6) $$\int G(\mathbf{r})\mathbf{u}_S(\mathbf{x}-\mathbf{r},t)\,\mathrm{d}^3\mathbf{r} = 0$$

cutoff wavenumber $k_c = \pi/\Delta$

filtered equations

(7)
$$\frac{\partial u_{Fi}}{\partial x_i} = 0$$

(8)
$$\frac{\partial u_{Si}}{\partial x_i} = 0$$

(9)
$$\frac{\partial u_{Fi}}{\partial t} + \frac{\partial (u_j u_i)_F}{\partial x_j} = \nu \frac{\partial^2 u_{Fi}}{\partial x_j \partial x_j} - \frac{1}{\rho_{00}} \frac{\partial p_F}{\partial x_i}$$

(10)
$$\frac{\partial (u_j u_i)_F}{\partial x_j} = \frac{\partial [u_{Fj} u_{Fi}]}{\partial x_j} + \frac{\partial (u_{Sj} u_{Si})_F}{\partial x_j}$$

(11)
$$\frac{\partial (u_{Sj} u_{Si})_F}{\partial x_j} = \frac{\partial (u_j u_i)_F}{\partial x_j} - \frac{\partial [u_{Fj} u_{Fi}]}{\partial x_j}$$

residual stress tensor $\tau_{Sij} = (u_i u_j)_F - u_{Fi} u_{Fj}$

residual kinetic energy $e = \frac{1}{2} \left[(u_i u_i)_F - u_{Fi} u_{Fi} \right]$

anisotropic residual stress tensor $\tau_{sij} = \left[(u_i u_j)_F - u_{Fi} u_{Fj} \right] - \frac{1}{3} q_S^2 \delta_{ij}$

modified filtered pressure $\tilde{p}_F = p_F + \frac{2}{3} e$

(12)
$$\frac{\partial u_{Fi}}{\partial t} + u_{Fj} \frac{\partial u_{Fi}}{\partial x_j} = \nu \frac{\partial^2 u_{Fi}}{\partial x_j \partial x_j} - \frac{1}{\rho_{00}} \frac{\partial \tilde{p}_F}{\partial x_i} - \frac{\partial \tau_{sij}}{\partial x_j}$$

TKE

(13) $$\frac{\partial e}{\partial t} + u_{Fj}\frac{\partial e}{\partial x_j} = \mathcal{P} + \mathcal{B} + \mathcal{D} - \varepsilon$$

(14) $$\mathcal{P} = -(u_{Si}u_{Sj})_F \frac{\partial u_{Fi}}{\partial x_j}$$

(15) $$\mathcal{B} = \frac{g}{\vartheta_{00}}(w_S\vartheta_s)_F$$

(16) $$\mathcal{D} = \frac{\partial}{\partial x_i}[-K_m\frac{\partial e}{\partial x_i}]$$

(17) $$\varepsilon = C\frac{e^{3/2}}{l}$$

where $l = \Delta$ for unstable conditions, $l = \Delta f(R_g)$ for stable cond.

parameterisation

(18) $$S_{Fij} = \frac{1}{2}\left(\frac{\partial u_{Fi}}{\partial x_j} + \frac{\partial u_{Fj}}{\partial x_i}\right)$$

(19) $$\mathcal{S}_F = 2\left(S_{Fij}S_{Fij}\right)^{1/2}$$

(20) $$\tau_{sij} = -2K_S S_{Fij}$$

(21) $$K_S = l_S^2 \mathcal{S}_F = (C_S\Delta)^2 \mathcal{S}_F$$

(22) $$\mathcal{P} \equiv -\tau_{sij}\, S_{Fij} = 2K_S S_{Fij} S_{Fij} = K_S \mathcal{S}_F^2/2$$

$\mathcal{P} > 0$: kinetic energy flux from resolved to unresolved scales.

two limits

- inertial subrange: $\Delta < L$. Being $l_S \sim \Delta$, $\mathcal{S}_F \sim \varepsilon^{1/3}\Delta^{-2/3}$ and $K_S \sim \varepsilon^{1/3}\Delta^{4/3}$
- Reynolds eqs. limit: $\Delta \gg L$. Thus $\mathbf{u}_F = \overline{\mathbf{u}}$, $\mathbf{u}_S = \mathbf{u}'$.

(23) $$\tau_{s12} = -K_S \frac{\mathrm{d}u_{F1}}{\mathrm{d}x_2} = -l_S^2 \left|\frac{\mathrm{d}u_{F1}}{\mathrm{d}x_2}\right| \frac{\mathrm{d}u_{F1}}{\mathrm{d}x_2}$$

(24) $$\overline{u_1 u_2} = -K_m \frac{\mathrm{d}\overline{u_1}}{\mathrm{d}x_2} = -l_m^2 \left|\frac{\mathrm{d}\overline{u_1}}{\mathrm{d}x_2}\right| \frac{\mathrm{d}\overline{u_1}}{\mathrm{d}x_2}$$

in the limit $\Delta/L \to \infty$ $K_S = K_m$ and $C_S = l_m/\Delta$

SBL simulations

from Beare et al. (2006)

initial/boundary conditions as in Cuxart et al. (2006)

the SBL is similar to Nieuwstadt (1984): moderate stability.

isotropic grid: $\Delta = 12.5,\ 6.25,\ 3.125,\ 2,\ 1\ m$

SBL height h from $\overline{u'w'}(h)/\overline{u'w'}|_0 = 0.05$

potential temperature, wind

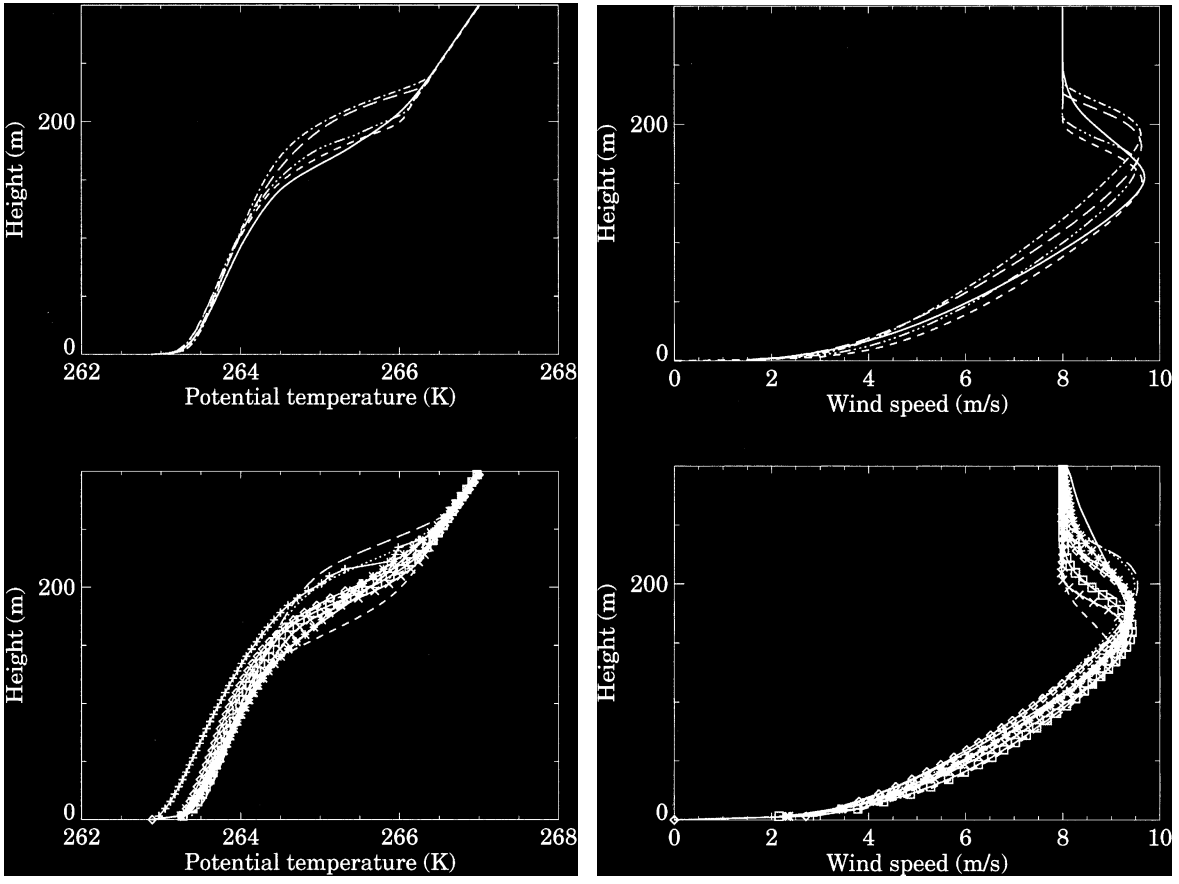

top: $\Delta = 2\ m$; bottom: $\Delta = 6.25\ m$

$R_b \sim 0.16 \div 0.23$ for $30 < z < 100\ m$ and $100 < z < 150\ m$ fairly consistent with Nieuwstadt (1984)

fluxes

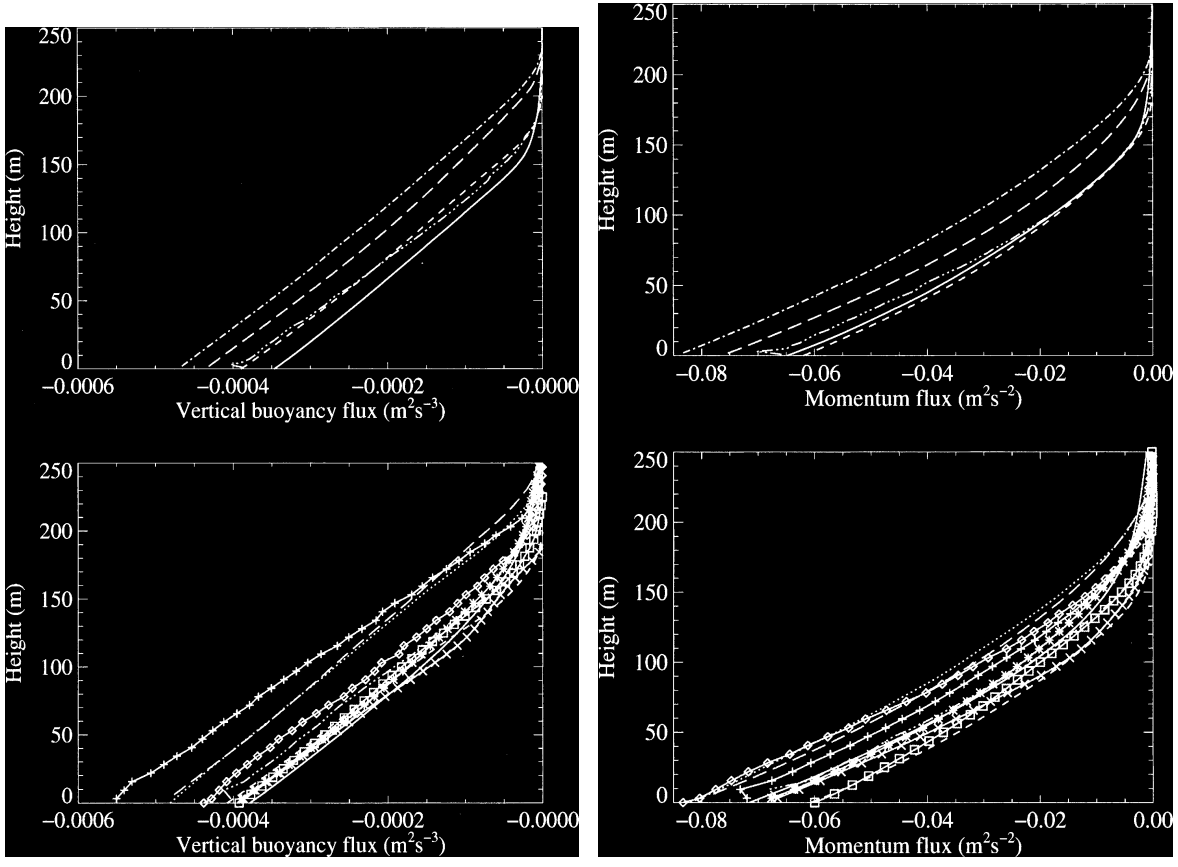
Height (m)
250
200
150
100
50
0
−0.0006
−0.0004
−0.0002
−0.0000
Vertical buoyancy flux (m²s⁻³)
Momentum flux (m²s⁻²)
−0.08
−0.06
−0.04
−0.02
0.00

scaled eddy diffusivities

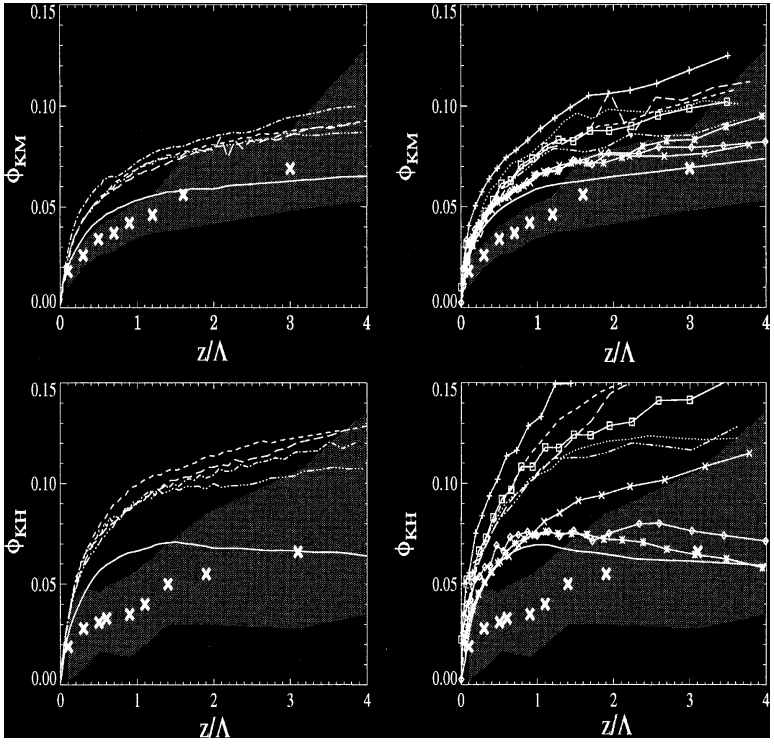

left: $\Delta = 2\ m$; right: $\Delta = 6.25\ m$

observations from Nieuwstadt (1984): $K_m(z/\Lambda)$, constant for large z/Λ.

$K_m = \tau/[(\,\mathrm{d}\overline{u}/\,\mathrm{d}z)^2 + (\,\mathrm{d}\overline{v}/\,\mathrm{d}z)^2]^{1/2}$ $\Phi_{km} = K_m/(\Lambda\tau^{1/2})$

fluxes

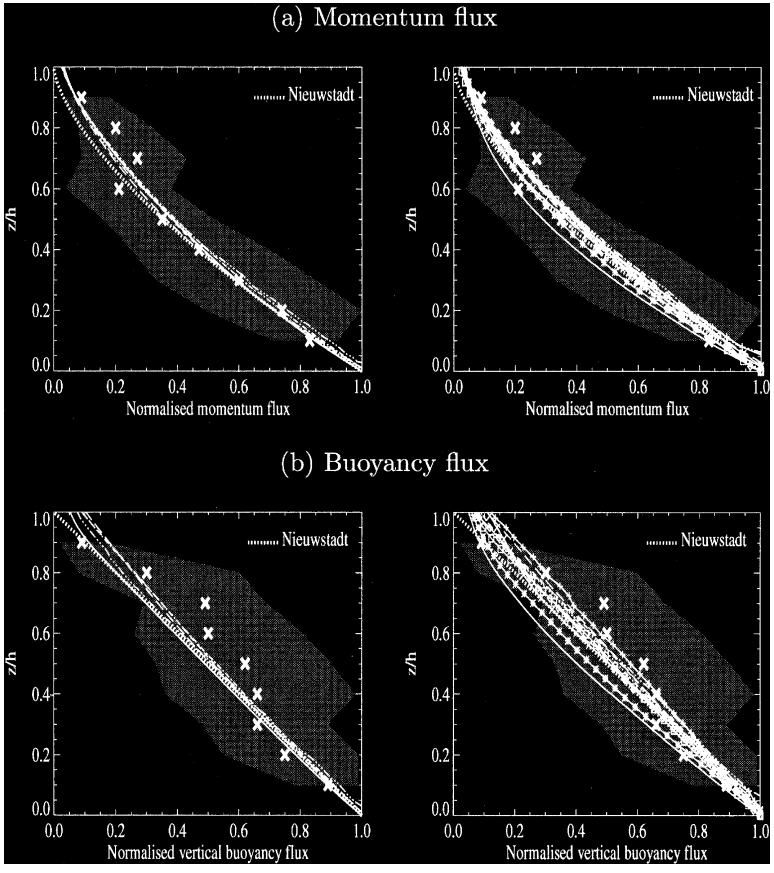
(a) Momentum flux
Nieuwstadt
z/h
Normalised momentum flux
Nieuwstadt
z/h
Normalised momentum flux
(b) Buoyancy flux
Nieuwstadt
z/h
Normalised vertical buoyancy flux
Nieuwstadt
z/h
Normalised vertical buoyancy flux

CBL simulation

from Sullivan and Patton (2011): CBL simulations at different resolutions:

- 32^3 grid points $=> \Delta_x = 160m$, $\Delta_z = 64m$
- ...
- 1024^3 grid points $=> \Delta_x = 5m$, $\Delta_z = 2m$

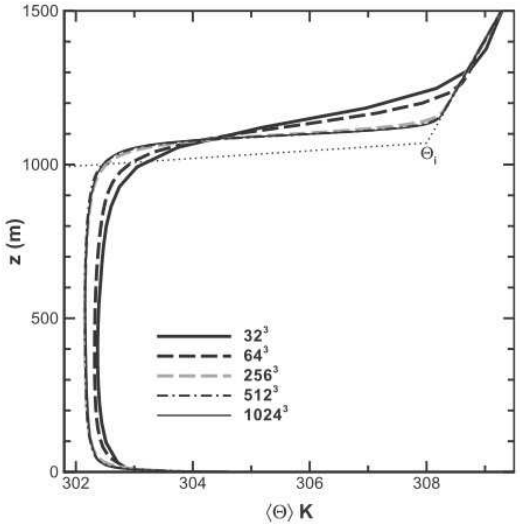

FIG. 2. Vertical profile of virtual potential temperature $\langle\tilde{\theta}\rangle$ for varying mesh resolution. Note all simulations are started with the same three-layer structure for virtual potential temperature θ_i, indicated by the dotted line.

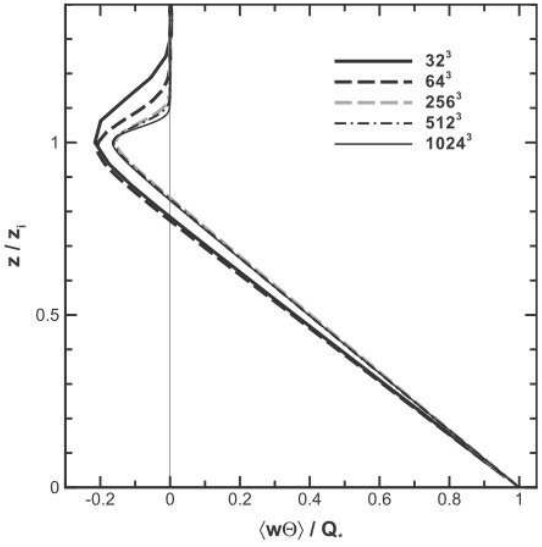

FIG. 3. Vertical profile of total temperature flux $\langle\tilde{w}''\tilde{\theta}'' + \mathbf{B}\cdot\hat{\mathbf{k}}\rangle/Q_*$ for varying mesh resolution.

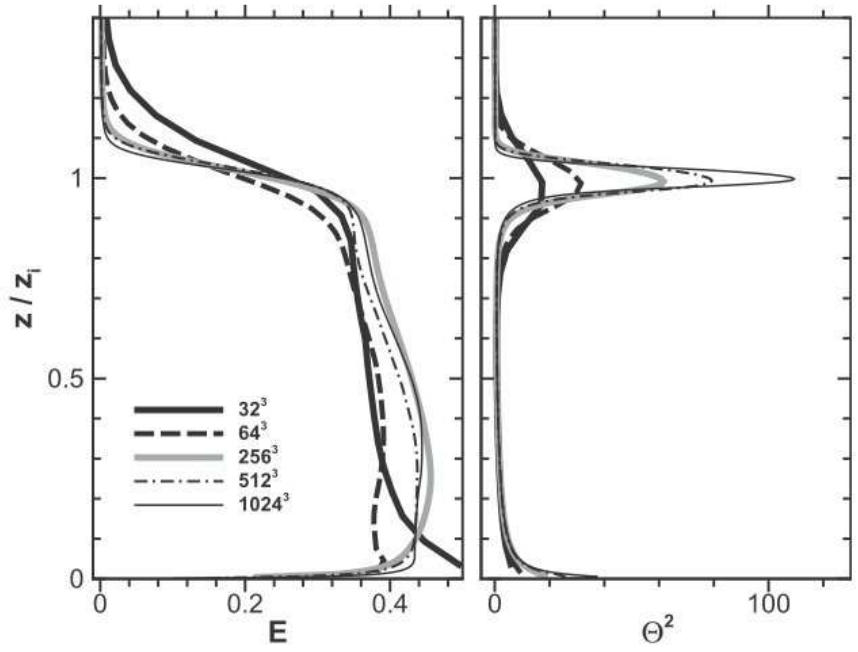

FIG. 5. Effect of mesh resolution on the (left) total turbulent kinetic energy (TKE) and (right) total temperature variance Θ^2. TKE is normalized by w_*^2 and the temperature variance is normalized by $\Theta_* = Q_*/w_*$.

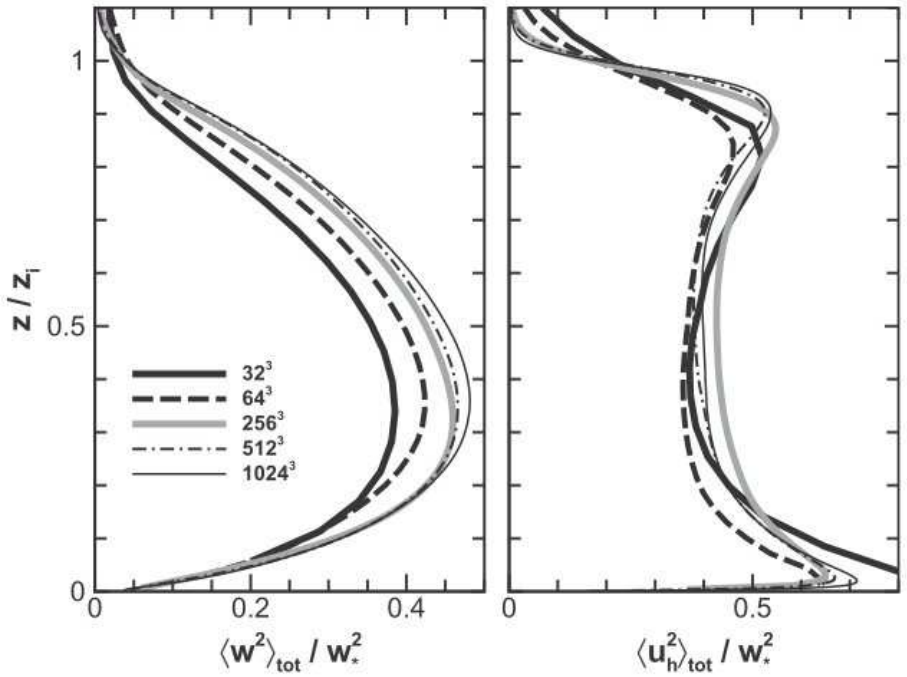

FIG. 6. Total variance (resolved plus SGS contributions) of the (left) vertical and (right) horizontal velocities. The horizontal variance u_h is the sum of the u and v components; see definition below (9).

spectra

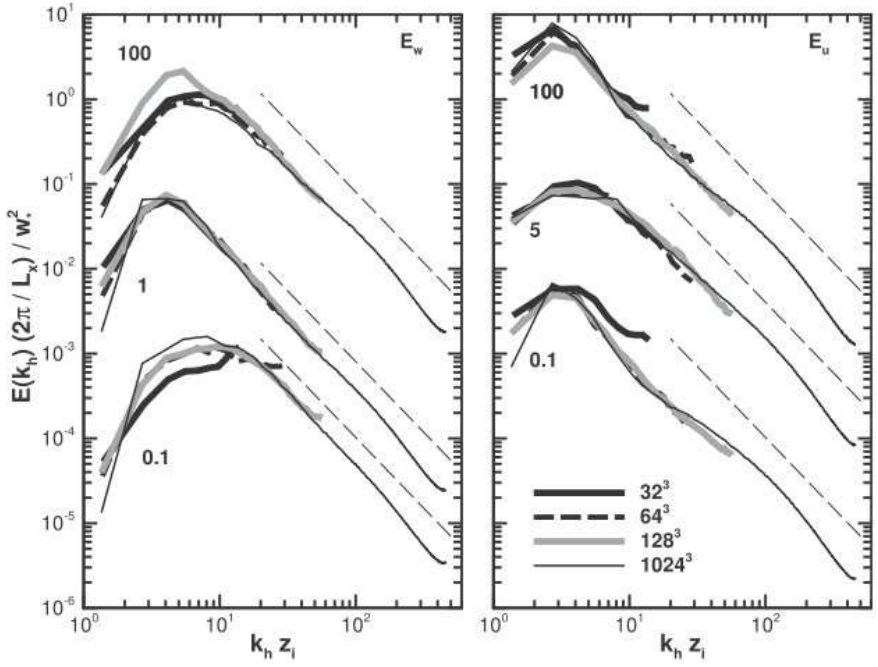

FIG. 7. Two-dimensional energy spectra of (left) vertical velocity w and (right) horizontal velocity u in the PBL for varying meshes. The spectra are functions of the magnitude of the horizontal wavenumber vector $k_h = |\mathbf{k}|$. The groups of spectra at the top, middle, and bottom in each plot correspond to the heights $z/z_i = 0.9$, 0.5, and 0.1, respectively. For clarity, the spectral amplitudes in each group are multiplied by the numerical factor on the left-hand side of the plot. The dashed line has slope $k_h^{-5/3}$.

spectra

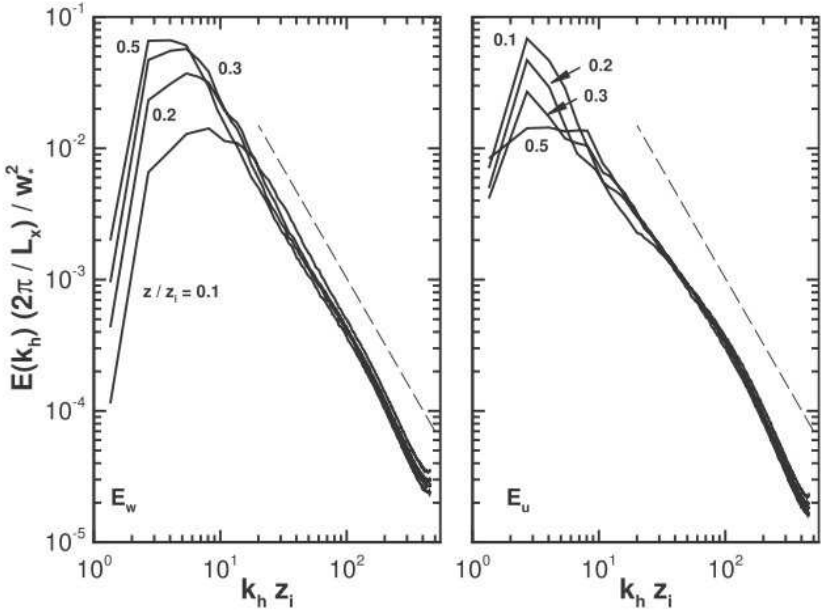

FIG. 8. Two-dimensional energy spectrum of (left) vertical velocity w and (right) horizontal velocity u near the lower boundary at various heights $z/z_i = 0.1, 0.2, 0.3$, and 0.5 for a simulations with 1024^3 grid points. The dashed line has slope $k_h^{-5/3}$.

skewness

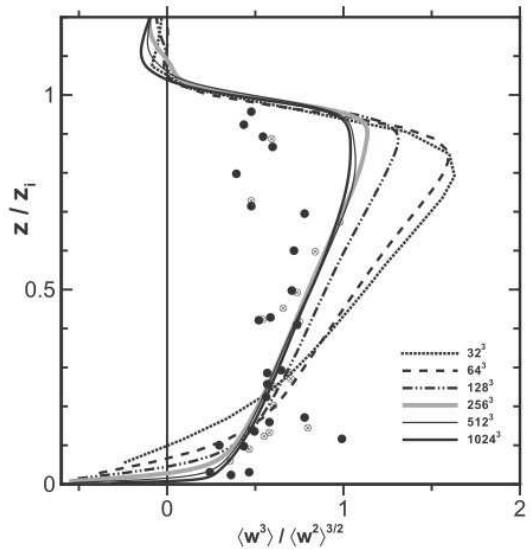

FIG. 9. Effect of mesh resolution on resolved vertical velocity skewness $S_{\overline{w}}$. The lines legend indicates the mesh size of the various simulations. The skewness is computed using the resolved (or filtered) vertical velocity field $\overline{w} = \overline{w}''$. The observations are taken from the results provided in Moeng and Rotunno (1990).

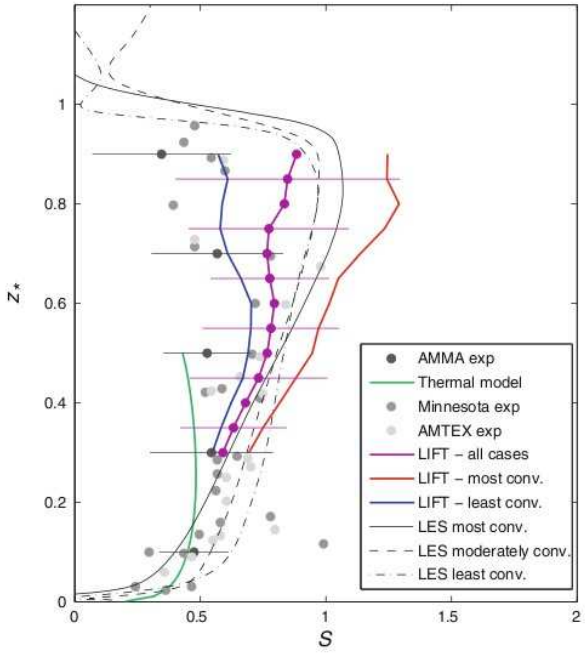

Fig. 5 Profiles of vertical velocity skewness in the CBL. The *symbols* are observations from previous experiments, as described by Moeng and Rotunno (1990). The *black circles* intersected with *horizontal lines* (which indicate the standard deviation of the measurements) are from AMMA (Redelsperger et al. 2006), the *dark grey circles* are from the Minnesota experiment (Wyngaard 1988), the *light grey circles* are from AMTEX (Lenschow et al. 1980) and the *coloured lines* are the averaged LIFT observations (*the horizontal magenta lines* through the *magenta circles* are the standard deviations of the LIFT observations). The *thin lines* are LES results (Sullivan and Patton 2011) and the *green line* is the thermal model of S

w field

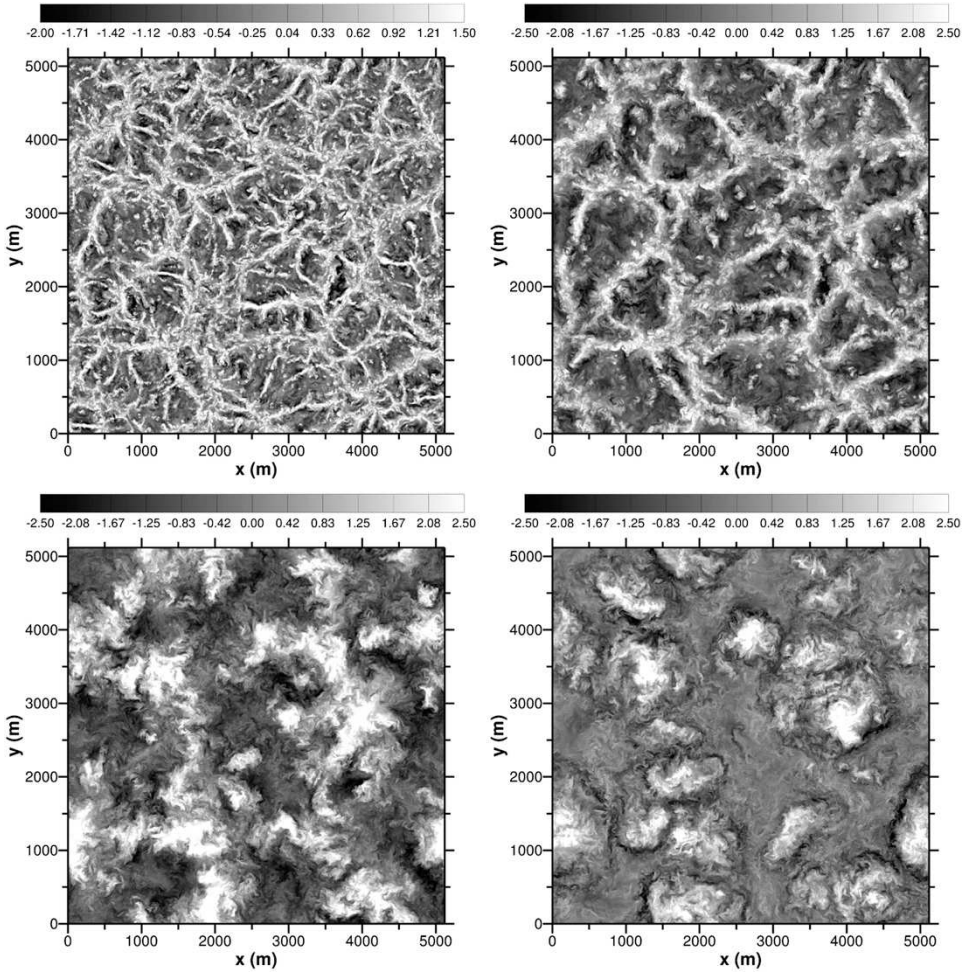

top left: $z/h = 0.04$; top right: 0.1; bottom left: 0.5; bottom righ: 0.9

CBL simulation and dispersion

Antonelli (pers. comm.): numerical code as in Antonelli and Rotunno (2007).
$h = 1000m$, $w_* = 2m/s$, $\Delta_{x,y} = 32\ m$, $\Delta_z = 15.5\ m$, $\varepsilon = C_\varepsilon/2^{3/2}\ q_S^3/\Delta$

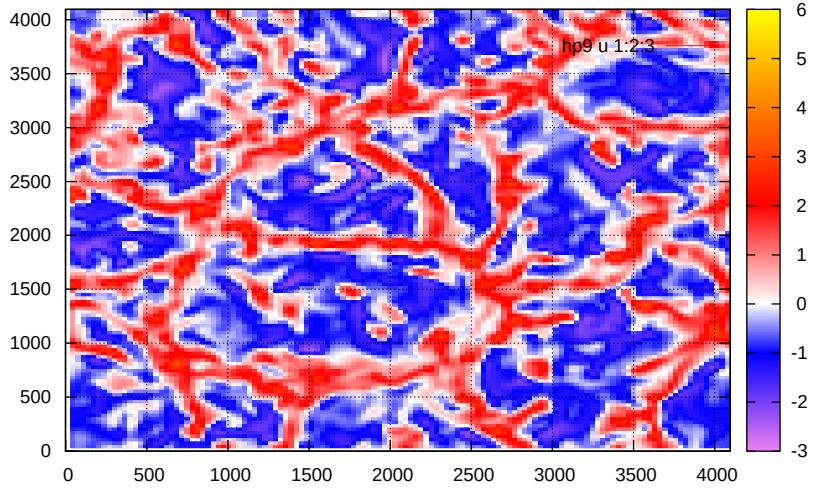

Vertical velocity in the plane $x - y$ at the source height $z_s = 150\ m$. Updraught in red, downdrought in blue. Source centers are located in the crossings of the grid.

ε, TKE, T_L

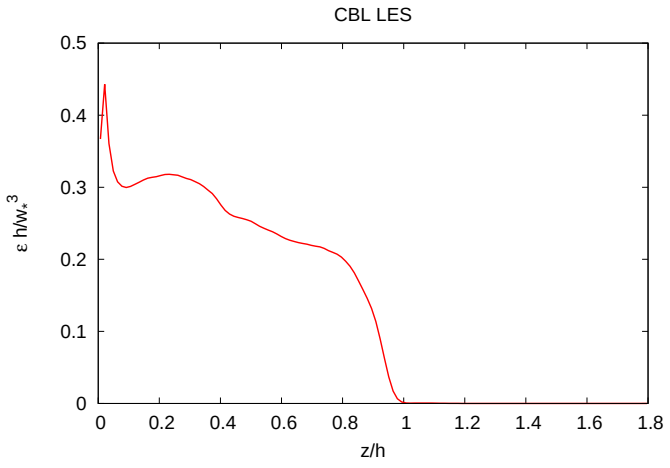

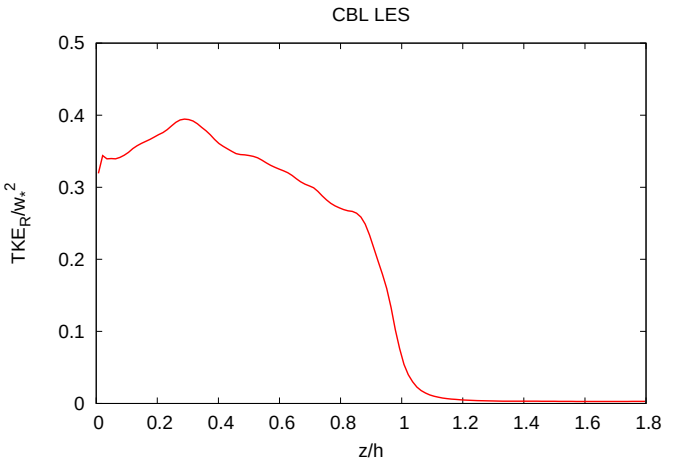

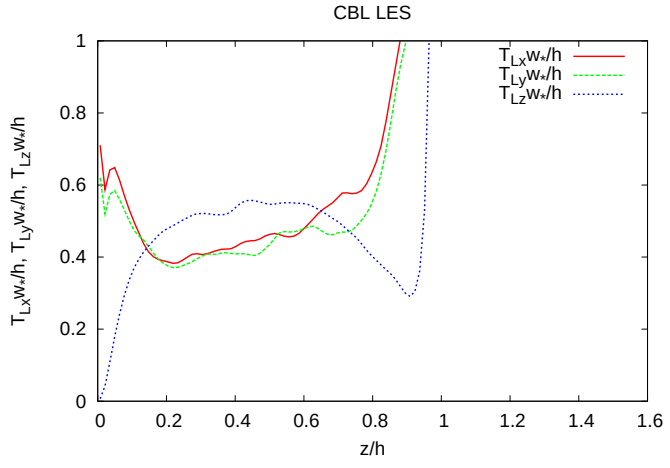

dissipation rate; TKE resolved, Lagrangian time scales derived as

$\tau_{Li} \equiv 2 < u_i'^2 > /(C_0 \varepsilon)$

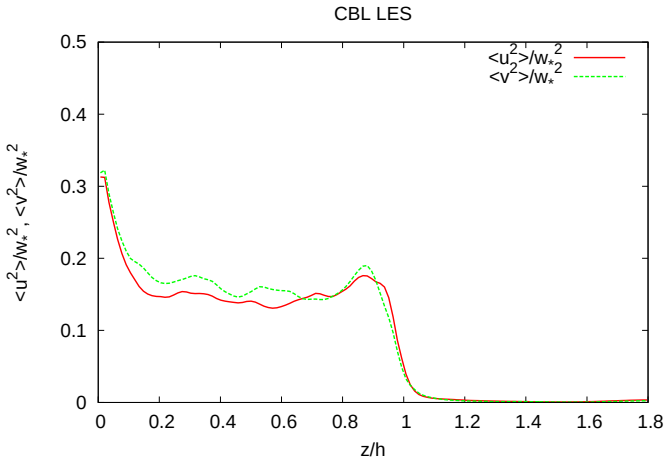

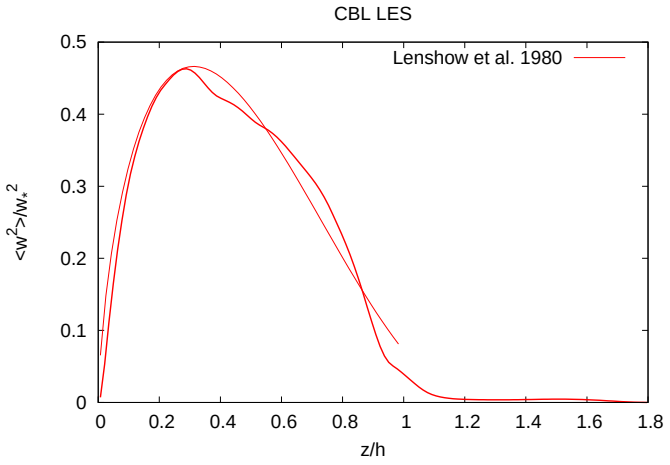

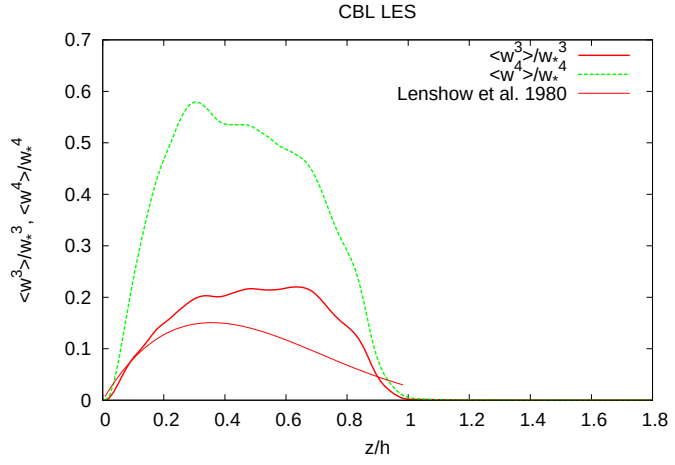

horizontal velocity variances, vertical velocity variance, skewness and kurtosis.
Thin continuous lines: parameterisations from Lenschow et al. (1980)

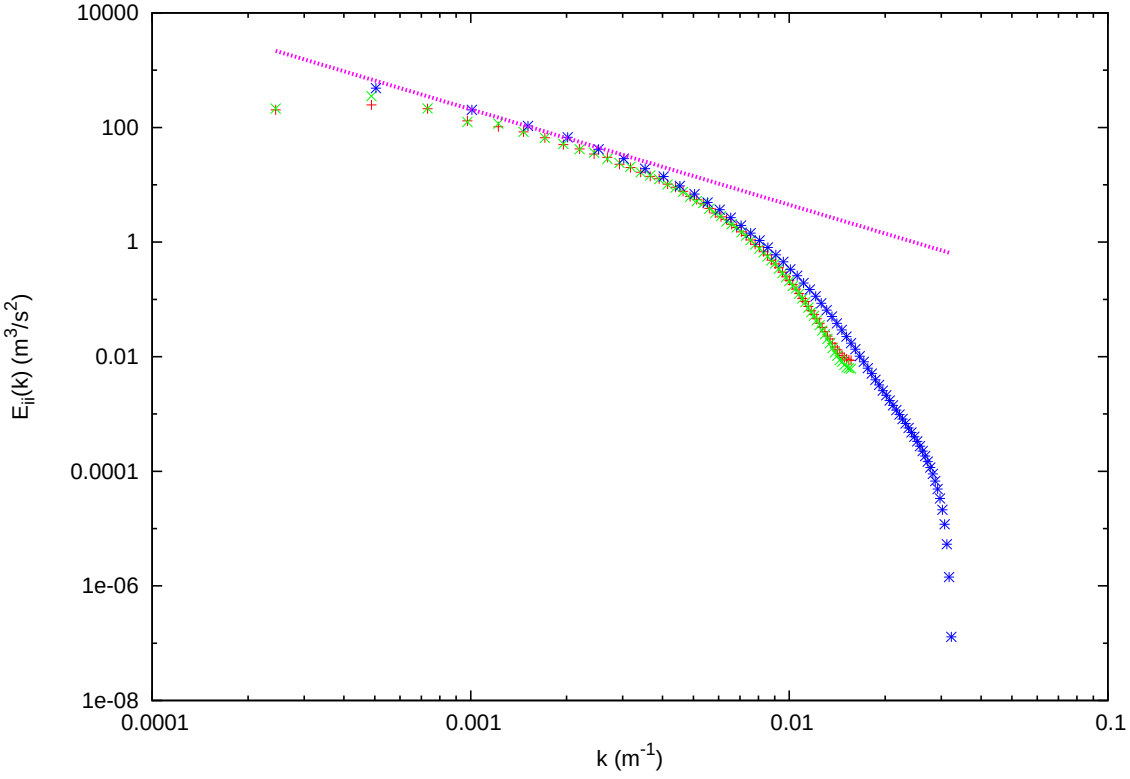

note the cut-off at wavenumbers of order Δ^{-1}

dispersion simulations in CBL

observations from Weil et al. (2002): a laboratory CBL

lateral dispersion

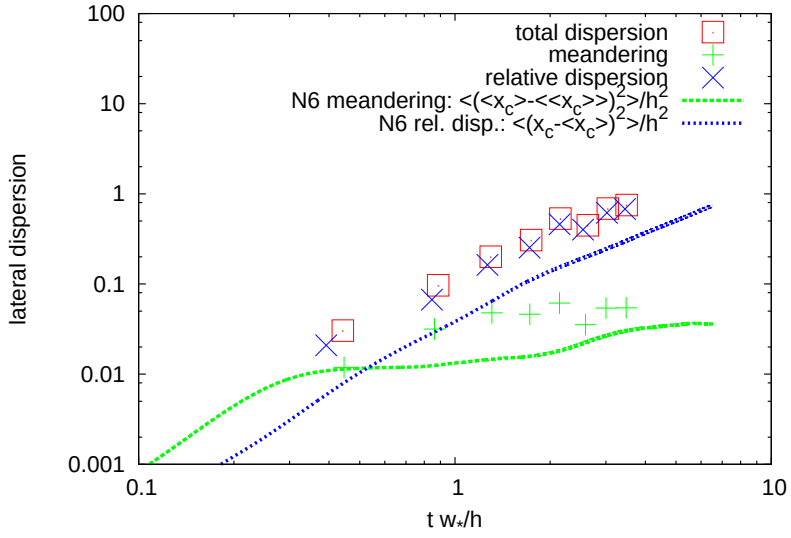

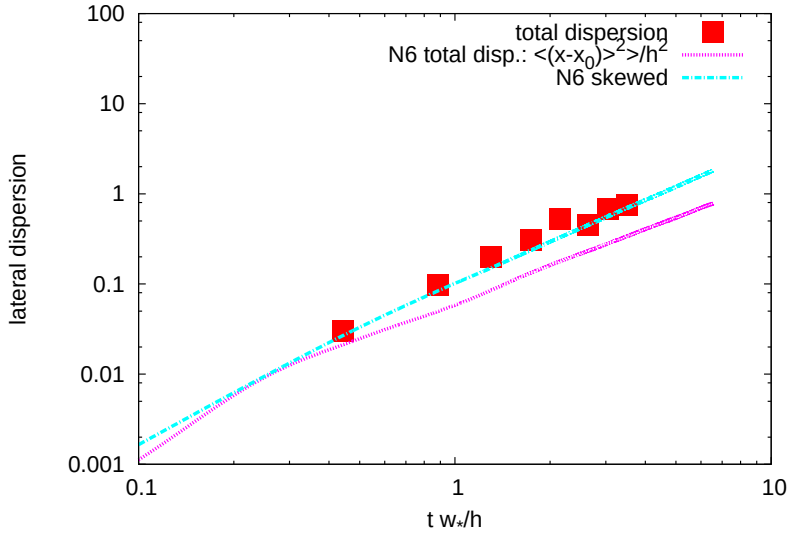

vertical dispersion

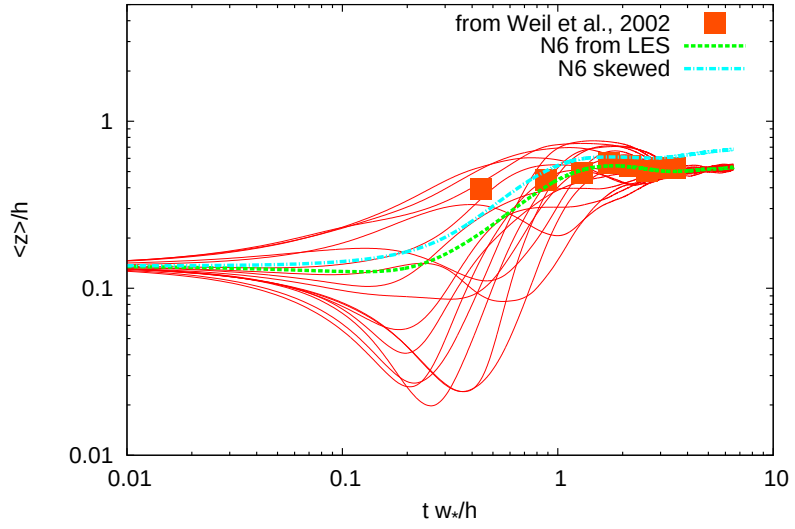

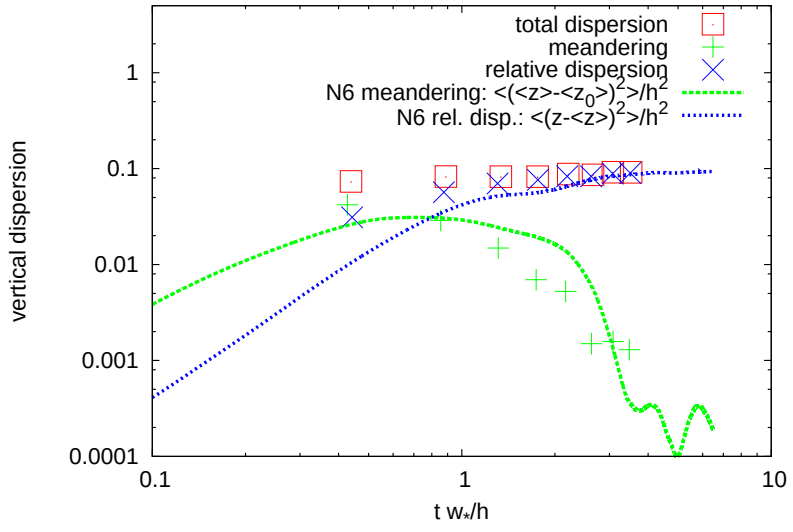

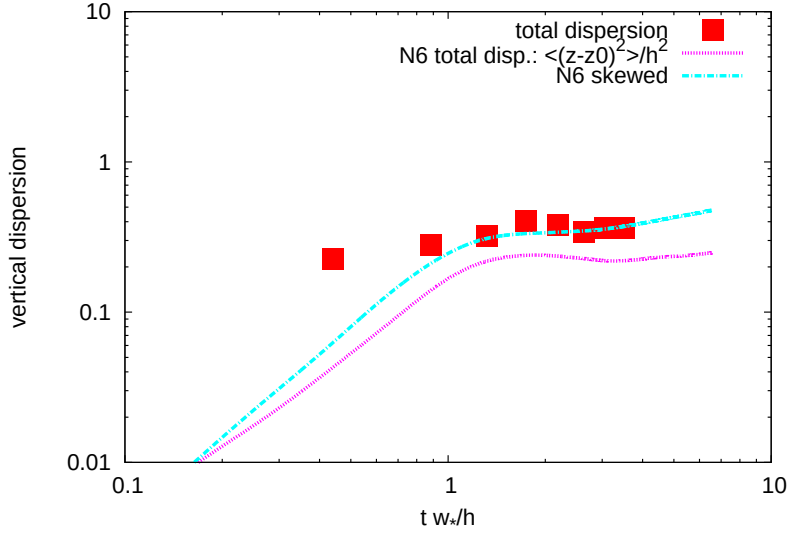

References

Antonelli, M. and R. Rotunno, 2007: Large-eddy simulation of the onset of the sea breeze. *J. Atmos. Sci.*, **64**, 4445–4457.

Beare, R. J., M. K. Macvean, A. A. M. Holtslag, J. Cuxart, I. N. Esau, J.-C. Golaz, M. A. Jimenez, M. Khairoutdinov, B. Kosovic, D. Lewellen, T. S. Lund, J. K. Lundquist, A. Mccabe, A. F. Moene, Y. Noh, S. Raasch, and P. P. Sullivan, 2006: An intercomparison of large-eddy simulations of the stable boundary layer. *Boundary-Layer Meteorology*, **118**, 247–272.

Cuxart, J., A. A. M. Holtslag, R. J. Beare, E. Bazile, A. Beljaars, A. Cheng, L. Conangla, M. Ek, and F. Freedman, 2006: Single-column model intercomparison for a stably stratified atmospheric boundary layer. *Boundary-Layer Meteorol.*, **118**, 273–303.

Lenschow, D. H., J. C. Wyngaard, and W. T. Pennel, 1980: mean field and second moment budgets in a baroclinic convective boundary layer. *Journal of Atmospheric Sciences*, **37**, 1313–1326.

Nieuwstadt, F. T. M., 1984: The turbulent structure of the stable, nocturnal boundary layer. *J. Atmos. Sci.*, **41**, 2202–2216.

Sullivan, P. J. and E. G. Patton, 2011: The effect of mesh resolution on convctive boundary layer statistics and structures generated by Large-Eddy Simlation. *Journal of Atmospheric Sciences*, **68**, 2395–2414.

Weil, J. C., W. H. Snyder, R. E. Lawson, jr., and M. S. Shipman, 2002: Experiments on buoyant plume dispersion in a laboratory convection tank. *Boundary-Layer Meteorol.*, **102**, 367–414.